


8-2014

USE OF UNMANNED AERIAL VEHICLES (UAV) FOR URBAN TREE INVENTORIES

Brian Ritter

Clemson University, britter@g.clemson.edu

Follow this and additional works at: https://tigerprints.clemson.edu/all_theses

 Part of the [Forest Sciences Commons](#), [Geographic Information Sciences Commons](#), and the [Natural Resources Management and Policy Commons](#)

Recommended Citation

Ritter, Brian, "USE OF UNMANNED AERIAL VEHICLES (UAV) FOR URBAN TREE INVENTORIES" (2014). *All Theses*. 1890.
https://tigerprints.clemson.edu/all_theses/1890

This Thesis is brought to you for free and open access by the Theses at TigerPrints. It has been accepted for inclusion in All Theses by an authorized administrator of TigerPrints. For more information, please contact kokeefe@clemson.edu.

USE OF UNMANNED AERIAL VEHICLES (UAV) FOR
URBAN TREE INVENTORIES

A Thesis
Presented to
The Graduate School of
Clemson University

In Partial Fulfillment
of the Requirements for the Degree
Master of Science
Forest Resources

by
Brian A. Ritter
August 2014

Accepted by:
Dr. Christopher J. Post, Committee Chair
Dr. Elena Mikhailova
Dr. Larry Gering

ABSTRACT

In contrast to standard aerial imagery, unmanned aerial systems (UAS) utilize recent technological advances to provide an affordable alternative for imagery acquisition. Increased value can be realized through clarity and detail providing higher resolution (2-5 cm) over traditional products. Many natural resource disciplines such as urban forestry will benefit from UAS. Tree inventories for risk assessment, biodiversity, planning, and design can be efficiently achieved with the UAS. Recent advances in photogrammetric processing have proved automated methods for three dimensional rendering of aerial imagery. Point clouds can be generated from images providing additional benefits. Association of spatial locational information within the point cloud can be used to produce elevation models i.e. digital elevation, digital terrain and digital surface. Taking advantage of this point cloud data, additional information such as tree heights can be obtained. Several software applications have been developed for LiDAR data which can be adapted to utilize UAS point clouds. This study examines solutions to provide tree inventory and heights from UAS imagery. Imagery taken with a micro-UAS was processed to produce a seamless orthorectified image. This image provided an accurate way to obtain a tree inventory within the study boundary. Utilizing several methods, tree height models were developed with variations in spatial accuracy. Model parameters were modified to offset spatial inconsistencies providing statistical equality of means. Statistical results ($p = 0.756$) with a level of significance ($\alpha = 0.01$) between measured

and modeled tree height means resulted with 82% of tree species obtaining accurate tree heights. Within this study, the UAS has proven to be an efficient tool for urban forestry providing a cost effective and reliable system to obtain remotely sensed data.

Keywords: Aerial Photography, Arboriculture, Clemson University, GIS, LiDAR, Remote Sensing, Tree Height, Tree Inventory, UAVS, UAV

DEDICATION

This study is dedicated to my wife Laurie and son Zachary. They have supported me throughout my time at Clemson and they deserve a large amount of credit, for they have provided beyond measure patience, support and love to help me succeed.

ACKNOWLEDGEMENTS

I wish to thank my committee: Dr. Christopher Post, Committee Chairman, Dr. Elena Mikhailova, and Dr. Lawrence Gering for their help and support during development and completion of this study. Thanks to Clemson University Facilities Services for providing funding, and to Paul Minerva, Clemson University Arborist, for insight and support. I acknowledge and thank Russell Buchanan, GIS Specialist, for providing field work, photogrammetry assistance and data entry. Technical Contribution No. 6162 of the Clemson University Experiment Station.

TABLE OF CONTENTS

	Page
TITLE PAGE	i
ABSTRACT.....	ii
DEDICATION	iv
ACKNOLWLEDGMENTS	v
LIST OF FIGURES	viii
LIST OF TABLES.....	ix
CHAPTER	
I INTRODUCTION	1
II MATERIALS AND METHODS	8
Study Area	8
UAV Aerial Imagery	8
Imagery Processing.....	8
Tree Inventory.....	9
Field Analysis	9
Generation of DEM, DTM, and CHM.....	9
Calculate Tree Heights.....	11
Statistical Analysis.....	11
III RESULTS AND DISCUSSION.....	12
UAV Imagery	12
Imagery Processing	12
Tree Inventory	15
Field Analysis.....	15
Generation of DEM, DTM, and CHM	16
Calculate Tree Heights	21
Statistical Analysis	22

Table of Contents (Continued)

IV	CONCLUSION.....	25
V	APPENDIX.....	51
	Glossary	51
	Flow Diagram for LASTool Processing	56
	REFERENCES	57

LIST OF FIGURES

Figure	Page
1 General classification of UAV's.....	26
2 LiDAR returns when laser pulses hit the ground and trees	27
3 Study boundary where UAV will be implemented.....	28
4 Ground control station during launch of UAV	29
5 Ground control software during actual UAV mission	30
6 Example of tonal imbalances and spatial alignment inaccuracies occurring after image processing.....	31
7 Completed orthomosaic of study boundary created from UAV images.....	32
8 Results of tree inventory created on orthomosaic from UAV images	33
9 Screen capture of tree inventory attribute table after field data was added	34
10 Spatial comparison of Dronemapper point cloud and tree inventory point	35
11 TiFFS output using LiDAR point cloud with tree inventory points	36
12 TiFFS output using UAV point cloud with tree inventory points	37
13 Fusion canopy height model results with tree inventory points	38
14 Screen capture of tree inventory attribute table with interpolated elevations from UAV point cloud DEM and DTM models.....	39

LIST OF TABLES

Table	Page
1 Unmanned aerial vehicle (UAV) products related to urban forest uses	40
2 Benefits of having a tree inventory	41
3 American Society of Photogrammetry and Remote Sensing (ASPRS) standard LiDAR point classes	42
4 Aerial coverage by UAV flights in summer 2013	43
5 Comparative analysis between UAV and field tree inventory techniques for summer 2013 flight mission	44
6 Flow design for processing UAV point cloud using LASTools to classify points and create DTM and DEM.....	45
7 Statistical results comparing measured and estimated tree heights based on tree inventory location to closest LiDAR point	46
8 Statistical comparison of grass and building values to develop a scale factor for pixel conversion to actual elevation heights	47
9 Statistical results of comparing measured and estimated tree heights using Agisoft/LASTool point cloud analysis interpolated to tree inventory points.....	48
10 Statistical comparison of means for individual tree species that have measured and estimated tree heights	49

CHAPTER 1

INTRODUCTION

Unmanned aerial vehicles (UAV) or unmanned aircraft vehicle systems (UAVS) have in recent years, established their presence across the world even though they have been around since the 1920's (Arjomandi, 2007). Comprising 93% of aerial reconnaissance during World War I, balloons were the forerunner of the modern day UAV (Blom, 2010). Primarily developed for the military, advancement in technologies has lead to increased UAV applications within natural resource disciplines. Monitoring, surveillance, mapping and three dimensional (3D) modeling are the primarily natural resource UAV applications. Little of the potential has been realized in civilian UAV applications (Merino et.al. 2006). In the United States, existing/unclear regulatory restrictions governing UAV/UAVS use has limited commercial use. Within natural resource disciplines, research is ongoing and new opportunities are rapidly emerging as the technology advancements continue. Despite the regularity uncertainty, UAV use is showing extensive value within natural resources and agriculture communities.

The UAV is an aircraft that can be controlled from the ground maintaining a level flight pattern in the absence of an onboard pilot (Elias, 2012). There are many different designs for UAV air frames which fall into two general categories; fixed and rotary winged (Figure 1) (Elias, 2012; DIY, 2013). With varying design in body and wing type general classifications can be further divided by performance parameters which include: weight, payload, longevity, range, motor type, maximum altitude and speed (Remondino et. al. 2011). Additionally alternate characteristics for classification can include: cost and

wing span (Arjomandi, 2007). Autonomous, air, hand and mechanical launch methods vary with size and type of UAV. The UAV size limits the type of application and sensor carried onboard. Sensor development within consumer digital camera markets has seen many technological advances resulting in much smaller, affordable and effective sensors for smaller UAV platforms. Technological advances in digital cameras, geographical positioning systems (GPS), and autopilots allowed the use of smaller UAV's as platforms for remote sensing. Autopilots with onboard GPS aid in flight control, positioning of data being collected and even landing, resulting in ease of use and autonomous flight. Data collected while in flight can be directly stored on the aircraft or sent in real time back to ground control station (DIY, 2013)

Sensors on UAV's can produce an array of remotely sensed products. True color UAV orthophotography results in imagery with higher resolution (2 – 3 cm) and detail compared to traditional aerial imagery. Hyperspectral or multi-spectral imagery can be acquired from onboard UAV sensors. (Johnston et. al, 2003) Near Infrared (NIR) filters can be used to modify standard digital camera sensors resulting in vegetative monitoring products (Hunt, et. al, 2010). Thermal sensors allow for detecting temperature changes across the landscape (Rudol and Doherty, 2008). Development efforts are ongoing to fit Light Detection and Ranging (LIDAR) sensors on smaller UAV's (Wallace, 2012). In addition, full motion videos with real time data acquisition are possible using current technologies (Eugster and Nebiker, 2008).

UAV applications are in their infancy, however many applications are beginning to emerge. Vegetative health monitoring, precision agriculture, urban forestry, emergency

management, biological and traffic monitoring represent current application areas for the UAVs. Once legislative and regulatory factors in the United States are clarified, civilian applications of UAV's will become more prevalent. Modern UAV systems provide; low cost, high resolution imagery, currency of information, repeatability, short turnaround processing, mobility, reliability and an ease of use system (Laliberte et. al. 2008, Rango and Laliberte, 2010).

National Air Space (NAS) in the United States is governed by the Federal Aviation Administration (FAA). Civilian and commercial UAV's are limited in their application until new FAA rules can be developed. A detailed look at regulation and control of UAV use has begun due to increased civilian and commercial interests. In 2006, the FAA produced a document, "Unmanned Aircraft Operations in the National Airspace System", to detail special considerations towards use of a UAV within government, police, emergency management and university research. This is limiting the commercial/civilian growth of the UAV in the United States not only from its use but through research and development as companies are reluctant to move forward with regulatory uncertainty. Congress has increased the FAA budget to include funds to develop a UAV program. In February 2012, an appropriation was signed by President Obama and with financial support included mandates to streamline permits for UAV use and rule development (Mitchell, 2012). The FAA Modernization and Reform Act of 2012; details the requirements for the FAA to integrate UAV into the NAS by fiscal year 2015. In July 2012, the FAA released a fact sheet detailing its current stance on commercial use. The primary concern of FAA is focused on safety and they are considering the need for

integrated sense and avoid technology in UAV's. Privacy, national security, and GPS signal interference have factored into the decision by the FAA to limit UAV civilian and commercial applications. (GAO, 2012)

In natural resources, the urban forest is well suited for small UAV applications. UAV generated products for urban forestry can be used in many ways (Table 1). Urban forest management objectives are dictated by human use of the areas around trees. To understand how people use the urban forest and to determine tree diversity, it is important to create a spatial tree inventory. Tree diversity across the landscape can be identified with accurate inventories that detail forest characteristics (Rowntree, 1988). An indirect benefit of inventory analysis with the UAV is the collection and archive of aerial imagery for future temporal comparison. The affordable repeatability of acquiring UAV imagery offers the opportunity to complete spatiotemporal analysis to detect change over time. Remotely sensed data is ideal for detecting urban forest spatial patterns to map this change (Jomaa et. al, 2008). Traditional aerial photography methods may be limited in this respect because of the high cost of obtaining repeated imagery. Multi-temporal data can be collected by the UAV that will provide effective comparisons to provide understanding in landscape change and monitoring (Zhou and Wang, 2011). Inventory and spatial comparisons will provide valuable information of urban forest structure, diversity, and management. This information will lead to more effective management decisions.

Urban forest management begins with a tree inventory. Tree inventories provide information as to tree diversity, location, condition, size and species. They also provide

positive benefits to communities and jurisdictions (Table 2). Tree inventories are an essential component of developing an urban forest management plan. Inventories represent urban forest conditions at the time of data collection. Urban forests are dynamic with natural and man-made changes occurring often and inventories require updating on a regular basis. There are several ways to develop tree inventories with each having its own set of advantages and disadvantages. Economic considerations may dictate which methods are used for obtaining a tree inventory (NCFS, 2014).

Urban forest inventories have data collected depending on the primary motivation for the inventory. Typically, standard information that is collected from each tree includes: species, diameter, condition, maintenance needs, location (x, y coordinate) and growing conditions (canopy, soil type/volume, and moisture regimes) (NCFS, 2014). As part of an urban tree inventory, tree risk assessment is typically included. Management of tree risk is designed to mitigate both basic and complex urban infrastructure to identify potential for tree failure. Urban forest managers have the responsibility to identify varying tree risk levels present and to manage them in accordance to acceptable risk. Tree risk involves inspection and assessment of the risk trees pose to property or human injury (Pokorny et. al, 2003). Tree risk assessment can be divided into three levels; Level 1- limited visual inspection, Level 2- complete visual inspection, and Level 3- advanced assessment (ISA, 2013). Tree risk identifies the potential for failure and environmental conditions contributing to failure along with target analysis. In the urban forest, tree failure could result in significant damage to human health and property. (Ellison, 2005)

Light Detection and Ranging (LiDAR) uses light pulsed from a laser to measure distance to the earth's surface (Figure 2). Highly accurate three dimensional information regarding the earth's surface and objects on the surface can be obtained from LiDAR information (NOAA, 2013). Forest inventory, urban planning, landscape ecology, floodplain mapping, hydrologic modeling, geomorphology are some of the examples of how LiDAR data is being utilized (Chen, 2007). Using LiDAR has key advantages: it can be quickly collected, provides high sample density, collected in dense forest, collected day or night, and contains no geometric distortion (ESRI, 2014). A limiting factor to temporal acquisition of LiDAR is high acquisition cost (Chen, 2007). LiDAR data can be processed to determine vertical canopy structure and individual tree 3D modeling (Wang et. al, 2008). LiDAR data is in the form of a point cloud and when classified can produce results in the form of digital terrain models (DTM), digital elevation models (DEM) and canopy height models (CHM) (Yunfei et. al, 2008, ESRI, 2014). The Log ASCII Standard (LAS) file format is used to interchange LiDAR data between users. This file type is binary and maintains specific LiDAR characteristics while reducing complexity found in generic ASCII file structure. The LAS format is flexible to allow for customization within specific applications using an LAS Domain Profile (ASPRS, 2012). Each point in the LiDAR data set is classified to define object types encountered by laser pulses. Using classification codes (LAS 1.1 or LAS 1.2 or LAS 1.3) standardization is achieved to define classification values (Table 3). Delineation of ground and high vegetation points can be converted to raster data to determine tree heights using tools within ArcGIS software (ESRI, 2014). In contrast to

traditional LiDAR data acquisition, UAV generated imagery can be processed using multi-view stereopsis, to produce a point cloud similar to LiDAR. These point clouds can be processed using LiDAR methods resulting in DEM, DTM, and CHM products. (Harwin and Lucieer, 2012)

It is hypothesized that UAV products (imagery and 3D point cloud) can be used in place of traditional data to obtain tree inventories and heights. Objectives of this study are to: 1) evaluate the efficacy of a small UAV for routine urban aerial photo acquisitions in urban forestry, 2) produce spatially-referenced aerial photo orthomosaics from a UAV, 3) produce a tree inventory from UAV imagery, 4) use 3D point cloud from UAV imagery to develop a model that will accurately produce tree height values.

CHAPTER 2

MATERIALS AND METHODS

Study Area

Clemson University lies in the southwest corner of Pickens County in northwest South Carolina. This land grant university was founded in 1889 from a private gift of Thomas Clemson and was formally opened in 1893. Today the main campus covers 566 ha with an additional 12,949 ha of agriculture and forest land (Clemson, 2013). The purchase of a single winged vehicle called the SwingletCam (Figure 1) was acquired to aid in campus planning, and tree inventory. On the campus of Clemson University, deployment of a UAV occurred in October 2012. This study will be conducted across the main campus located in Clemson, SC (Figure 3).

UAV Aerial Imagery

Multiple missions were conducted between July and October 2013 (Table 4) to evaluate operational procedures and acquisition of aerial images. Missions were planned using strategic landing/take off zones to make efficient use of topography and photographic parameters. Geodetic ground control points (115) were established using geographic positioning system (GPS) to aid spatial referencing of images. Results were analyzed to evaluate altitude preferences, radio connectivity, image resolution/detail, and flight parameters.

Imagery Processing

Imagery was transferred from the UAV storage media to a computer for orthophoto processing. Images were geotagged with flight log data and processed to produce a

seamless orthorectified image for the study boundary. Open source, third party applications, and cloud based services were used to evaluate effectiveness in producing a seamless image derived from multiple temporal missions.

Tree Inventory

A tree inventory was conducted using the orthorectified images. A feature class representing the tree inventory was created based on UAV imagery using ArcGIS 10.1 software (ESRI, 2010). A heads up digitizing technique records tree locations as points through visual inspection of the high-resolution imagery. Each point corresponds to a single tree added in a feature class representing the overall tree inventory. Using pre-identified tree maintenance zones, the tree inventory process was conducted along a gridded pattern until each zone was complete. This process meets the requirement for Level 1 tree risk assessment.

Field Analysis

Field visits were conducted at each tree identified within the tree inventory. Species, diameter at breast height (DBH), and total tree height data was obtained. DBH was measured with a Biltmore stick (Black, 2014) and a Nikon Forestry Pro Model 8381 laser range finder (± 0.31 m) was used to obtain total tree heights. During field visits, visible defects were noted and recorded using a gps-enabled digital camera. The field analysis represents a level 2 tree risk assessment.

Generation of DEM, DTM, and CHM

Using LiDAR and UAV 3D point cloud data, a DEM, DTM, and CHM were generated. LiDAR data was used as a base line to validate UAV point cloud results.

Processing of both data sets was conducted using different approaches. Raw LiDAR data in LAS format were processed using the Fusion LIDAR viewing and analysis software developed by the United States Forest Service (USFS) to produce 3D terrain and canopy surface models (USFS, 2014). A Toolbox for LiDAR Data Filtering and Forest Studies (TiFFS) analyzes LiDAR LAS data processing them into terrain raster files (object height models (OHM), DEM, DSM), GIS feature classes (tree points, tree canopy polygons) and statistical raster files (kurtosis height, mean height, percent height, quad mean height, skewness height, standard deviation height). TiFFS utilize an automated routine that does not require pre-classified LIDAR point clouds for input. Having a more focused approach to obtaining forest information from LiDAR, TiFFS is designed to extract specific statistical related information in addition to terrain modeling (Globalidar, 2014). Among many tools that ArcGIS contains, LiDAR LAS files can be utilized to obtain terrain models. Additional toolsets can be used to analyze the terrain models and extract information such as tree heights. Using the UAV point cloud data may require additional software to prepare it for use. Converting the point cloud into LAS or ASCII format for input is typically required. There are products such as Microsoft Excel and Structured Query Language (SQL) Database for example, that can accomplish this conversion but due to the number of table rows (tens of millions for each mission) there may be limitations encountered due to large file sizes. Martin Isenburg has produced a set of tools (LASTools) specifically for LAS management (Rapidlasso, 2014). These tools can be used in a standalone graphical user interface, as a toolbox in ArcGIS or executed within operating system command line. This toolbox allows for quick and efficient

conversion of UAV point cloud data into LAS format. Agisoft is commercial based software that can process UAV images into a seamless orthorectified product. A single orthomosaic seamless image along with a 3D point cloud can be produced with Agisoft to develop a tree inventory and tree height model.

Calculate Tree Heights

Canopy Height Models (CHM) and object height models (OHM) derived from point cloud analysis can be used to directly obtain tree heights. Spatial interpolation at each tree location was used to extract these values to the tree inventory attribute table. ArcGIS 10.1 was used to spatially join this information to the point location files. Utilizing other tools in ArcGIS 10.1 (LASTools), the elevation models were developed and elevation values spatially joined to tree inventory points. These values were subtracted to obtain estimated tree heights.

Statistical Analysis

Statistical comparison of tree heights to field measured heights was conducted. Hypothesis testing of two means was used to validate the tree height model. If the null hypotheses are not rejected then the conclusion will show the means are equal and validate the tree height model. In the case of rejecting the null hypothesis, further statistical analysis was conducted to determine what factors may contribute to the rejection. Results can reveal if some tree species may not be subject to tree height modeling or other factors may cause spatial inconsistencies or inaccurate elevation values limiting accurate interpolated values to be obtained.

CHAPTER 3

RESULTS AND DISCUSSION

UAV Imagery

Nineteen UAV flights were flown between July and October 2013 (Table 4). A portable ground control station (Figure 4) was used to manage flight control with Emotion2 software (Figure 5). A total of 3466 color images with resolutions of 2.6-3.6 cm were collected from a typical altitude of 90 m. Between each image, 60% side lap and 40% forward lap parameters were used. This was needed to minimize distortional balances between images. The resolution obtained is useful to provide the scale needed to describe forest canopy and diversity variables within the forested landscape (Anderson and Gaston, 2013). During flight, images were stored on a secure digital (SD) card. Flight functions were provided with an onboard autopilot and GPS. Autonomous take off and landings provided ease of use. Ground control communication with the UAV was maintained using a 2.4 GHz radio link via a universal serial bus (USB) computer connection. The UAV functioned flawless at low altitudes and provided an effective solution for obtaining high resolution aerial photography.

Imagery Processing

Processing of images began with geotagging flight and camera information to each image. Geotagging was completed using a proprietary software (Post Flight Suite) supplied with the UAV. Geotagging adds information to the EXIF header that contains camera parameters and spatial x, y coordinate. A cloud based service (DroneMapper, <http://dronemapper.com>) was used to orthorectify and mosaic flights into a seamless

image. Only 2497 of the 3466 images were used for mosaic processing. Some images were dropped as they represented extended overlap between flights. In between flights with varying temporal periods introduced tonal imbalances, excessive shading (sun angle differences) and color inconsistencies. The extra images allowed for a selection process to choose the best image for orthorectification and minimization of potential visual inaccuracies. Prior to uploading flight images, ground control information was created using a GCP application supplied by DroneMapper. Two text files were needed to allow for georeferencing images to ground control. A file containing the name, x coordinate, y coordinate, z value and horizontal/vertical precision for each ground control point was used as a ground reference file (3D file). With DroneMapper's proprietary GCP software, images were analyzed to determine if any ground control was present. If present, the ground control point was selected with the computer mouse which correlated to the x, y pixel value on the image. A separate file (2D file) stored the name, x pixel, and y pixel values. The 2D file was edited changing the name to match its corresponding ground control point name. After all images were examined, both text files containing the ground control (3D file) and image control (2D file) information was uploaded with flight images. Due to the large number of images sent for processing, Dronemapper divided the image set into five processing blocks for increased efficiency. After processing by DroneMapper, products were returned which included orthorectified seamless image, DEM, DSM, and 3D point cloud for each block of images.

Upon receipt of DroneMapper products, each flight block was loaded into ArcGIS 10.1 for evaluation. In ArcGIS 10.1 additional mosaic tools were used to create a

seamless image of all flight blocks. Tonal imbalance (Figure 6) between flights occurred and with further analysis were not completely eliminated. A spatial grid (305 m x 305 m) was developed to clip original flight images. This process allowed for areas of tonal balance issues to be further edited by choosing flight overlaps that could be used to replace the tonal imbalances. From the tiled images, a new mosaic (Figure 7) was developed however tonal imbalances and color matching were not totally removed. The results from the additional processing improved the original product making it useful to obtain tree inventories.

Further investigation to enhance the image processing, a commercial application, Agisoft PhotoScan Professional Edition Ver. 1.0.4 (64bit) (<http://www.agisoft.ru/>) was used. Agisoft is designed to process photogrammetry data for orthorectification with additional functionality to produce an orthomosaic image, DEM, DTM and 3D point clouds. The same 2466 images used for DroneMapper processing were used as inputs to Agisoft creating a single orthorectified mosaic. This operation stressed computer resources (8 core processor, 32 gb RAM) during implementation. Results were examined in ArcGIS 10.1 and although minor tonal imbalances were present. Agisoft had overall better results over DroneMapper resulting in improved spatial accuracy and tonal balancing. DroneMapper minimized building distortion in contrast to Agisoft where buildings were misshaped and warped. In addition, a 3D point cloud was exported from Agisoft for utilization in tree height modeling.

Tree Inventory

The high resolution characteristics of the completed mosaic enhanced visual identification of individual trees for urban forest analysis and level 1 tree risk assessment. Using ArcGIS 10.1, individual trees were located and assigned a unique x/y coordinate by mouse click with the point added to the tree inventory feature class (Figure 8). Acquisition for both field and UAV tree inventory data was timed to calculate a total time per tree. The time per tree was multiplied by the total number of trees acquired during data collection for each method. The results (Table 5) reflected a realized savings of 29.3 days when using UAV methods. This information is invaluable as a way to offset limited resources for arboriculture applications.

Field Analysis

Field work is still ongoing to visit non-sampled trees. The goal is to visit all trees identified within the tree inventory. Currently, 1831 trees have been examined for level 2 risk assessment. Species, DBH, total height, and general condition were noted. DBH was obtained using a Biltmore stick (Black, 2014). Total tree heights were measured using a Nikon Forestry Pro Model 8381 range finder. A three point method was used to compute heights with the rangefinder. Ranging measurements were taken directly from three tree positions: eye level, base, and top of tree. Internally these measurements were used to return a tree height value. Data collected were field recorded pen and paper method. ArcGIS 10.1 was used to edit the tree inventory feature class, keycoding field data associated with each tree (Figure 9). A total of 57 unique tree species were

identified through field observations. Diversity among trees is represented by 31 genus and 46 species.

Generation of DEM, DTM, and CHM

Generation of elevation models was conducted using Agisoft and Dronemapper products. Models were derived utilizing TiFFS, Fusion, ArcGIS and LASTools. Each model was evaluated for spatial and tree height accuracies.

Dronemapper supplied DEM, DTM and point cloud files. The DEM and DTM were compared to LiDAR DEM. It was observed, pixel values for the UAV based DEM and DTM products were not true elevation values. It was surmised that these values were missing a scale factor to correlate with actual elevation values. In an attempt to develop a scale factor, a point grid was developed using the LiDAR and DroneMapper DEM pixel values. These were spatially assigned to each point in the grid. Using the field calculator in ArcGIS 10.1, a new attribute was assigned a scale up factor derived from dividing the LiDAR elevation by the pixel value. Points were then randomly selected and classified into grass (open flat areas) and buildings (top of building). The means of each classified group of points were looked at statistically to see if there were differences based on cover type. The result was used to scale the pixel value to represent actual elevation. The results, where successful for ground elevation (DEM) however, the scale factor was not valid to accurately assimilate height elevations.

The point cloud provided by DroneMapper included x, y and z values for each pixel in the mosaic imagery. Assuming the z value represents object height, the x and y values could be used to spatially locate each pixel. Through tools in ArcGIS 10.1, a raster

model representing the y value could be produced. Due to extremely large (millions) point cloud files, data preparation was necessary to use the files in ArcGIS. The X, Y Data tool requires a text or Microsoft Excel file to spatially locate each pixel. Excel has a 1,048,000 row limit so each point cloud file had to be parsed into smaller files. Each point cloud file can be programmatically split into manageable sizes then converted to excel format for processing. This task did not prove to be efficient due to the number of files produced and time needed for conversion. This method was processed at a smaller scale for testing. One flight was processed to produce a point file that could be spatially joined to tree inventory. Spatial inaccuracies occurred with actual tree inventory locations not in line with x, y generated points. In an attempt to correct spatial offsets, the near tool in ArcGIS 10.1 was used to select the closes elevation to a measured tree. It was found that the closest point was not always the correct one. In many instances, the correct pixel was farther away from the closest point. The neighborhood analysis (3 x 3) tool in ArcGIS 10.1 was used to evaluate the points. This method captured in many cases the correct pixel and the maximum value within each neighborhood could be used for tree height interpolation (Figure 10). This process contained variability across spatial extents and was not considered a feasible method without modification.

The LAS Toolkit (Rapidlasso, 2014) includes the txt2LAS tool. DroneMapper point cloud files were converted without parsing of data into a file similar to LiDAR. The new file was used to build a raster model representing the z value. A comparison was made against the LiDAR DEM. When compared to the LiDAR DEM, resulting point cloud z values were negative. This indicates it was representing elevations below the DEM. It

was concluded that the z value in DroneMapper's point cloud did not represent object height and were not in the same scale. More information needs to be gathered from DroneMapper as to methods and metadata before the point cloud can be used in tree height modeling.

Utilizing TiFFS proved to be user friendly with its automated process to take LAS files and create estimates of forest metrics. It was designed specifically to utilize LiDAR information to analyze forest structure. The outcome from TiFFS produced several results: DEM, DSM, OHM, ground and object LAS point cloud, and ESRI shapefiles representing crown, and trees. Interpolated tree height values are present in the attribute table and can be compared with tree inventory measured heights. Both LiDAR and DroneMapper point clouds were analyzed in TiFFS. Outcomes for both point clouds were compared to the tree inventory both visually and statistically. Spatial comparisons show inaccuracies in tree location for both LiDAR and UAV Dronemapper derived point clouds (Figure 11-12). The LiDAR results have a closer spatial relationship to inventory trees. Further investigation is needed to determine the cause for spatial inaccuracies; however it is hypothesized that map projections and projection transformations may be the cause of the inaccuracy.

Fusion (USFS, 2014) utilizes user developed command line files to produce canopy (CHM) and elevation models (DEM). LiDAR point clouds were processed using this method. CHM returned spatial correlation to tree inventory (Figure 13). Spatial interpolation at tree locations joined CHM elevations to tree inventory points. Measured tree heights were compared to CHM values statistically to determine equality. The

results were inconsistent across the tree inventory. Slight to moderate differences in tree heights were observed.

ArcGIS 10.1 provides tools designed for processing LiDAR point clouds. These tools were utilized to develop a DTM model. A DEM model was not needed, since one was provided with the LiDAR point cloud. Inconsistent point cloud classifications (only ground point's classified-LAS 2) were used to develop a DTM from vegetative classifications (LAS 1-first returns). The result was spatially interpolated to tree inventory points. Using the LIDAR (3.05 m x 3.05 m) derived DEM supplied with the LiDAR point cloud, the tree inventory revealed interpolated elevation values in like manner. A comparison of the DEM and DTM values concluded dissimilarity between measured and estimated tree heights. Statistical analysis was performed to determine equality. Measured and interpolated tree heights were considered equal if $p\text{value} < \text{level of significance (0.01)}$. Statistical results concluded that inequality existed across the study boundary. It was perceived that this result was not spatially explicit and elevation data was subdivided into tiles for statistical analysis. A pattern of discontinuity was found indicating that the model did represent object heights within certain spatial extents. There seems to be some indication that map projection, datum and unit transformation may have introduced error into the model. In addition it is hypothesized, that filtering of unclassified points during processing could have included outliers that skewed the results. In addition, the date of acquisition between LIDAR (2011) and UAV (2013) data could cause dissimilarity between elevations.

Agisoft was used to generate a seamless orthomosaic and 3D point cloud by using each UAV image (2497 total) in a six step process. The process aligned, built geometries, georeferenced, meshed, textured, and mosaicked the images into a single true color high resolution image and point cloud. The resulting image was an improvement over other results with no tonal imbalances and spatial accuracies within 10.5 cm of geodetic control. Some building distortion was present but did not distract from the trees. A point cloud containing x, y, z, Red (R), Green (G), Blue (B) values for each point was exported as a text file. LASTools was used to convert the text file into an unclassified LiDAR (. las) format. In Agisoft, to obtain increased spatial accuracy, native UAV map projection (WGS1984 Lat/Long) was used. To utilize LASTools, a conversion of the map projection was required to convert the point cloud file to UTM WGS 1984 Zone 17N. Due to point cloud file size (209⁺ million points) tiling was used to parse the file into smaller units for processing. Each file was batched processed (Table 6) to: tile, classify ground points, convert z values to true heights, and classify building/high vegetation points using default parameters built into each tool. A LASTool (las2DEM) for creating DEM's was used to convert the ground and high vegetation points into separate DSM and DTM models. These tools were utilized within an application developed in ArcGIS Model Builder to streamline LASTool utilization. A BAT file was created to enable LASTool to process all tiles in sequence for greater efficiency using a step value of 0.25 representing a 25 cm neighborhood for point processing. The ground DEM obtained increased accuracy for surface elevations as a result. To classify high vegetation into a DTM, only class 3, 4, and 5 were used in the "--keepclass" parameter to

exclude all other classified point while also using the “–extrapass” parameter to improve point processing. The result of executing the bat file inside the command line improved overall efficiency of executing. Output DEM and DTM for each tiled point cloud resulted in elevation values with a higher degree of spatial accuracy. The mosaic tool was used in ArcGIS to stitch all tiles into a single DEM and DTM for the study boundary. Once complete, elevations (DEM and DTM) could be interpolated and then compared to each tree within the inventory.

Calculate Tree Heights

The DEM, DTM, and CHM elevation models provided the basis to compare data layer elevation values to tree point locations and the associated measured tree height. The elevation models (DEM and DTM) were developed for both LiDAR and UAV point clouds. Ground elevation (DEM) was compared by subtracting from object height (DTM) values to create a layer (CHM) with the height of objects above ground level. Values from this height raster were added to the feature class for the point tree locations so that measured tree heights could be statistically compared with estimated heights. Filtering of the estimated heights was needed to remove erroneous values attributed to no data areas. Descriptive statistics were calculated on the filtered results for statistical analysis. Accuracy with this process is dependent upon the density of the point cloud, and the resulting elevation model.

Examining the outputs of the models tested, the DEM and DTM from LASTools provided the best results when compared to point cloud processing in Fusion or TIFF's. Dissimilar map projection units, spatial inaccuracies, temporal differences between data

collections and unclassified points caused varying levels of inaccuracy. UAV point cloud processing with LASTools reduced many of these inaccuracies. Tree heights were interpolated and incorporated as an attribute in the tree inventory feature class (Figure 14). Descriptive statistics were calculated on the filtered results for statistical analysis.

Statistical Analysis

Statistical comparisons were made between measured and estimated tree heights. Descriptive statistics for mean, N, and standard deviation calculated in ArcGIS 10.1, were used in a t-test calculator (GraphPad (<http://www.graphpad.com/quickcalcs/ttest1/>)) for p-value determination. Trees (27% of total inventory) with measured and estimated tree heights were used for comparison of means.

LiDAR derived CHM's results found that tree heights were not equal to measured tree heights ($p = 0.0001$) which was unexpected. LiDAR data was parsed into tiles to determine if this was spatially consistent across the study boundary. A neighborhood search for LiDAR values at varying distances was used to determine if position accuracy could have caused the poor height estimates with the LiDAR data. Statistical analysis (Table 7) for each tile shows there is an exception and spatial areas exist where tree heights are equal ($p > 0.01$). These results indicate that spatial inaccuracies between the CHM and tree location(s) provided inaccurate height results for certain spatial extents. It is concluded if spatial alignment issues can be resolved accurate tree height values could be interpolated.

The DEM and DSM provided from DroneMapper did not have a consistent scale factor to convert pixel value into a usable elevation value, which made it unusable for

estimating tree heights. A gridded method was used to construct a model to compare grass or open areas to building tops. If the scale factor for each classification is equal the derived scale then it could be used to convert pixel values. GraphPad was used to compare two means using a t-test. The results (Table 8) show that both scale factors are equal ($p = 0.056$). Further testing is needed to determine if the scale factor is valid for both the DEM and DSM models and if a variable scale factor would be necessary.

The results (Table 9) of LASTool processing of the Agisoft point cloud concluded at the level of significance ($\alpha = 0.01$) that the measured and estimated tree heights were equal ($p = 0.7641$). These statistical results show that using the point cloud from high resolution imagery can be accurate for tree height determination. Further statistical testing was performed stratifying the measured height sample to look at individual tree species. Individual species (70.2% of all species with measured heights) with $n > 1$ were tested to compare measured and estimated tree height means. This testing ($\alpha = 0.01$) show that 82% of individual species had equal means (Table 10). The 18% with unequal means include *Cornus florida*, *Ilex opaca*, *Lagerstroemia indica*, *Magnolia virginiana*, *Quercus alba*, *Pinus teada*, and *Thuja occidentalis*. Three species, *Pinus teada*, *Quercus alba* and *Thuja occidentalis* showed measured mean values higher (22%, 20% and 40% respectively) than estimated means. In contrast, *Cornus florida*, *Ilex opaca*, *Lagerstroemia indica* and *Magnolia virginiana*, showed higher estimated means (42%, 31%, 21%, and 54%, respectively).

Multiple statistical and physical characteristics were examined to determine factors that could have explained the seven species with unequal means. Plausible explanations

indicate that no single factor contributes to the error in height estimation. A combination of factors likely caused the error. Stratifying the data by species, an evaluation was conducted that revealed three characteristics: sparse point cloud, tree point proximity (< 5 m) to buildings and miss-classified/unclassified points as probable causes of error. When examining these factors, adjoining point values influenced estimated tree height results. Proximity to buildings caused estimated tree heights to increase while areas of little to no points (sparse point cloud) caused measured heights to be greater than estimated heights. Miss-classified and unclassified points could cause either height value to increase over the other and is dependent upon closest point to actual tree location. Additional analysis was conducted spatially adjusting (increased neighborhood size to 1 meter from 25 centimeters) DEM parameters in an attempt to increase accuracy among estimated heights. Statistical analysis for all species revealed at the level of significance ($\alpha = 0.01$) estimated and measured tree heights were still equal ($p = 0.9628$). Comparing the seven species with unequal means, statistically they remained unequal ($p = 0.0001$). It was observed that 71% of the individual species showed estimated height means were higher than measured means. For these species distance to buildings was the contributing factor as elevation points representing the building influenced (increasing) estimated tree height. The other 29% of species show mean measured heights greater than mean estimated heights. This was due to sparse point cloud and miss-classified points influencing (decreasing) estimated tree heights.

CHAPTER 4

CONCLUSION

Research objectives were to evaluate UAV implementation potential within the urban forest, build a tree inventory and develop a tree height model from an imagery derived point cloud. The UAV proved to be an effective tool to acquire high resolution imagery. Agisoft rendered orthomosaic photos that had high spatial and tonal accuracies. Findings include that ground control points are required to provide spatial accuracy needed for imagery and terrain model correlation to tree position(s). Tree inventory acquisition using the high-resolution UAV imagery and resulting point cloud was simple with increased efficiency resulting in time savings over traditional methods. Tree height model processing had varied results depending on software used. Future opportunities exist to uncover deficiencies related to height modeling within different software applications. Agisoft mosaic generation provided the best solution for image processing and point cloud extraction. LASTools proved to be effective in producing accurate tree heights ($p = 0.7641$) from UAV point clouds. Due to inequality with several individual tree species it is suggested that parameters for point cloud creation and classification needs user customization to account for factors contributing to their difference of means. This study has shown how the UAV can improve tree inventory workflows while generating a higher degree of visibility to assist in effective management decisions.

Figure 1 General classification categories of UAV's



Fixed Wing Swinglet Cam <http://www.sensefly.com/products/swinglet-cam>



Multicopter <http://diydrone.com/profiles/blogs/a-newbies-guide-to-uavs>

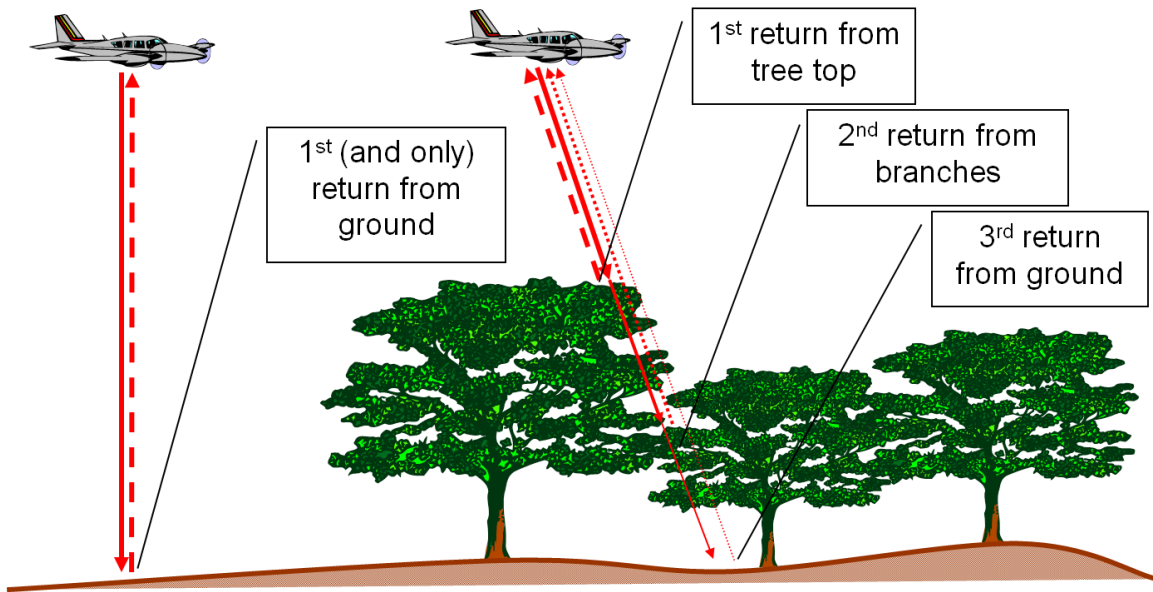


Figure 2 LiDAR returns when laser pulses hit the ground and trees (FRA, 2014)

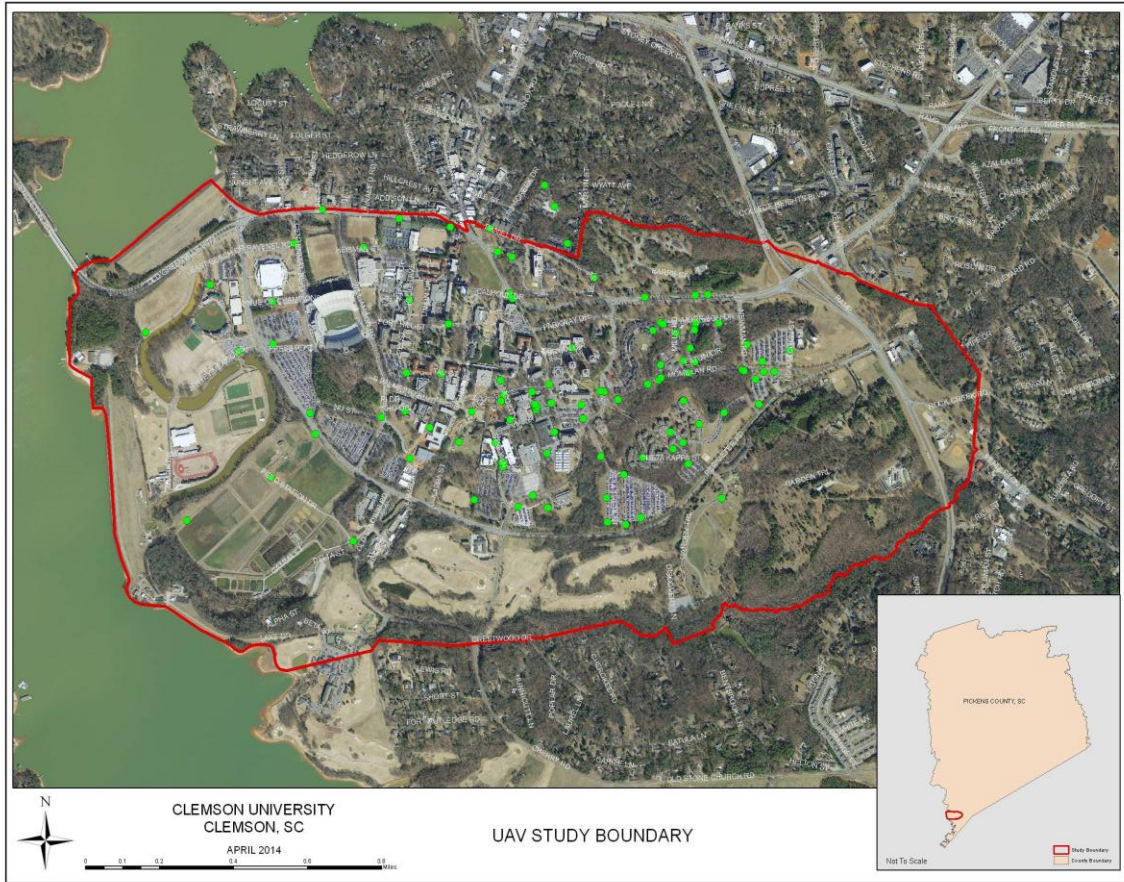


Figure 3 Study boundary used for UAV implementation to collect high resolution imagery for developing a tree inventory and tree height model. Green dots represent geodetic control locations



Figure 4 Ground control station for Sensefly Swinglet UAV. The control station provides continuous flight monitoring and UAV control

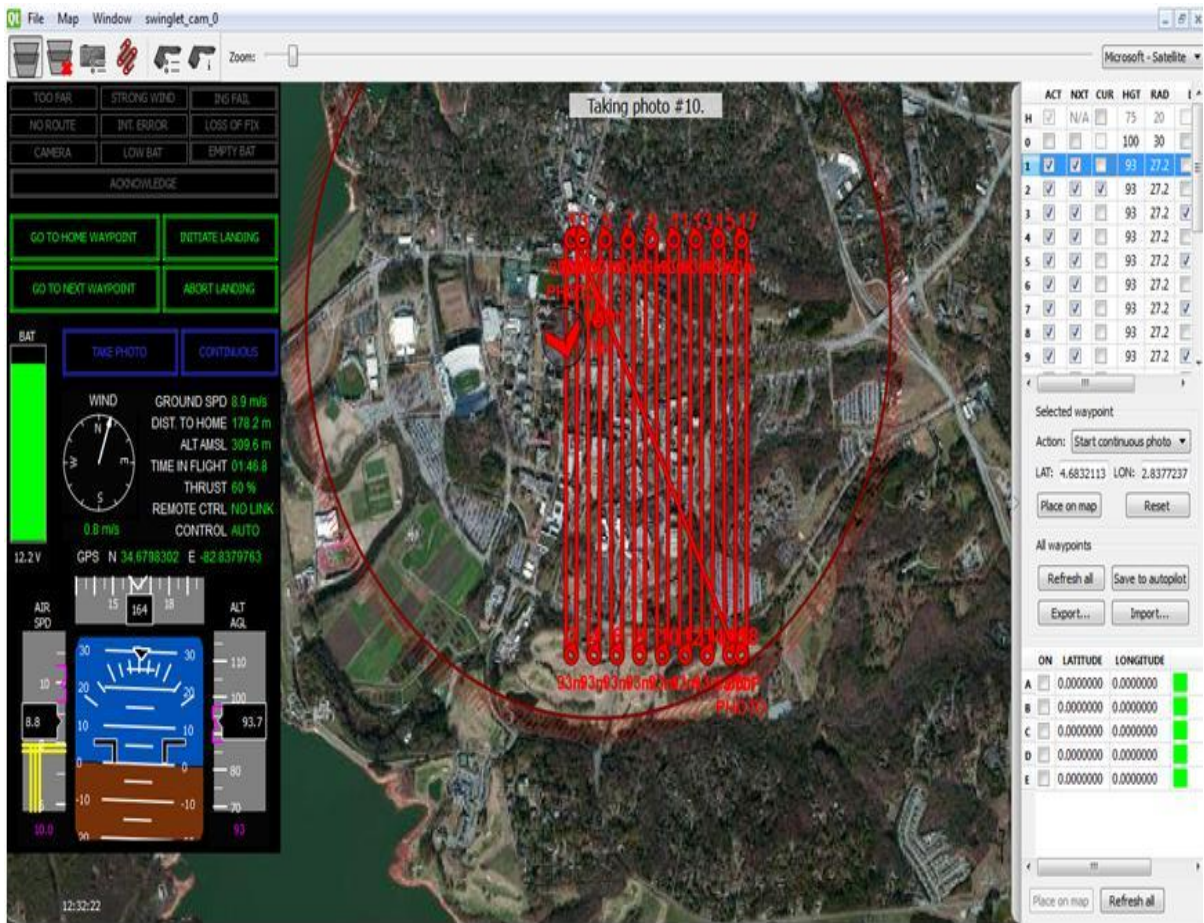


Figure 5 Screen capture of Emotion2 software (Sensefly, Inc.) during aerial photo mission. The screen contains flight controls, current mission parameters, communication limits, and flight path(s)



Figure 6 Tonal imbalances and spatial alignment inaccuracies occurring between flights following image processing



Figure 7 Completed georeference mosaic of Clemson University. This seamless orthomosaic was used for tree inventory acquisition



Figure 8 Tree inventory results using high resolution mosaic of Clemson campus

OBJECTID	GENUS	SPECIES	COMMON	DBH	HEIGHT	CROWND	LOC_VALUE	CONDITION	INSPE_ZONE	VALUE	OWNER	EDIT_USER	ZoneNum	Tree	TreeID	Tree_Code
12	Comus	florida	Flowering Dogwood	6.0	34.0	0.0	0	0	0	0	Facilities	RBuchanan	01	0012	010012	COFL
13	Comus	florida	Flowering Dogwood	6.0	34.0	0.0	0	0	0	0	Facilities	RBuchanan	01	0013	010013	COFL
14	Comus	florida	Flowering Dogwood	6.0	35.0	0.0	0	0	0	0	Facilities	RBuchanan	01	0014	010014	COFL
15	Comus	florida	Flowering Dogwood	5.0	33.0	0.0	0	0	0	0	Facilities	RBuchanan	01	0015	010015	COFL
16	Comus	florida	Flowering Dogwood	5.0	32.0	0.0	0	0	0	0	Facilities	RBuchanan	01	0016	010016	COFL
17	Comus	florida	Flowering Dogwood	5.0	32.0	0.0	0	0	0	0	Facilities	RBuchanan	01	0017	010017	COFL
18	Comus	florida	Flowering Dogwood	5.0	32.0	0.0	0	0	0	0	Facilities	RBuchanan	01	0018	010018	COFL
19	Comus	florida	Flowering Dogwood	6.0	25.0	0.0	0	0	0	0	Facilities	RBuchanan	01	0019	010019	COFL
20	Comus	florida	Flowering Dogwood	5.0	34.0	0.0	0	0	0	0	Facilities	RBuchanan	01	0020	010020	COFL
21	Comus	florida	Flowering Dogwood	8.0	30.0	0.0	0	0	0	0	Facilities	RBuchanan	01	0021	010021	COFL
22	Comus	florida	Flowering Dogwood	6.0	35.0	0.0	0	0	0	0	Facilities	RBuchanan	01	0022	010022	COFL
23	Comus	florida	Flowering Dogwood	8.0	33.0	0.0	0	0	0	0	Facilities	RBuchanan	01	0023	010023	COFL
24	Comus	florida	Flowering Dogwood	8.0	32.0	0.0	0	0	0	0	Facilities	RBuchanan	01	0024	010024	COFL
25	Comus	florida	Flowering Dogwood	3.0	13.0	0.0	0	0	0	0	Facilities	RBuchanan	01	0025	010025	COFL
26	Comus	florida	Flowering Dogwood	6.0	27.0	0.0	0	0	0	0	Facilities	RBuchanan	01	0026	010026	COFL
27	Comus	florida	Flowering Dogwood	6.0	25.0	0.0	0	0	0	0	Facilities	RBuchanan	01	0027	010027	COFL
28	Comus	florida	Flowering Dogwood	6.0	28.0	0.0	0	0	0	0	Facilities	RBuchanan	01	0028	010028	COFL
29	Comus	florida	Flowering Dogwood	5.0	27.0	0.0	0	0	0	0	Facilities	RBuchanan	01	0029	010029	COFL
30	Comus	florida	Flowering Dogwood	9.0	37.0	0.0	0	0	0	0	Facilities	RBuchanan	01	0030	010030	COFL
34	Magnolia	‡soulangeana	Saucer Magnolia	3.0	19.0	0.0	0	0	0	0	Facilities	RBuchanan	01	0034	010034	
37	Magnolia	‡soulangeana	Saucer Magnolia	4.0	19.0	0.0	0	0	0	0	Facilities	RBuchanan	01	0037	010037	
51	Betula	nigra	River Birch	16.0	58.0	0.0	0	0	0	0	Facilities	RBuchanan	01	0051	010051	BENI
55	Juniperus	virginiana	Eastern Red Cedar	19.0	38.0	0.0	0	0	0	0	Facilities	RBuchanan	01	0055	010055	JUVI
68	Acer	nigrum	Black Maple	10.0	38.0	0.0	0	0	0	0	Facilities	RBuchanan	01	0068	010068	ACNI
69	Acer	nigrum	Black Maple	11.0	41.0	0.0	0	0	0	0	Facilities	RBuchanan	01	0069	010069	ACNI
75	Ilex	opaca	American Holly	2.0	7.0	0.0	0	0	0	0	Facilities	RBuchanan	01	0075	010075	ILOP
76	Ilex	opaca	American Holly	2.0	7.0	0.0	0	0	0	0	Facilities	RBuchanan	01	0076	010076	ILOP
77	Ilex	opaca	American Holly	2.0	7.0	0.0	0	0	0	0	Facilities	RBuchanan	01	0077	010077	ILOP
78	Ilex	opaca	American Holly	2.0	7.0	0.0	0	0	0	0	Facilities	RBuchanan	01	0078	010078	ILOP
79	Ilex	opaca	American Holly	2.0	7.0	0.0	0	0	0	0	Facilities	RBuchanan	01	0079	010079	ILOP
80	Ilex	opaca	American Holly	2.0	7.0	0.0	0	0	0	0	Facilities	RBuchanan	01	0080	010080	ILOP
81	Lagerstroemia	indica	Crape myrtle	4.0	9.0	0.0	0	0	0	0	Facilities	RBuchanan	01	0081	010081	LAIN
82	Lagerstroemia	indica	Crape myrtle	3.0	7.0	0.0	0	0	0	0	Facilities	RBuchanan	01	0082	010082	LAIN
83	Lagerstroemia	indica	Crape myrtle	3.0	9.0	0.0	0	0	0	0	Facilities	RBuchanan	01	0083	010083	LAIN
84	Lagerstroemia	indica	Crape myrtle	3.0	9.0	0.0	0	0	0	0	Facilities	RBuchanan	01	0084	010084	LAIN
85	Lagerstroemia	indica	Crape myrtle	3.0	9.0	0.0	0	0	0	0	Facilities	RBuchanan	01	0085	010085	LAIN
86	Lagerstroemia	indica	Crape myrtle	3.0	8.0	0.0	0	0	0	0	Facilities	RBuchanan	01	0086	010086	LAIN
87	Lagerstroemia	indica	Crape myrtle	3.0	12.0	0.0	0	0	0	0	Facilities	RBuchanan	01	0087	010087	LAIN
88	Lagerstroemia	indica	Crape myrtle	4.0	8.0	0.0	0	0	0	0	Facilities	RBuchanan	01	0088	010088	LAIN
89	Lagerstroemia	indica	Crape myrtle	4.0	10.0	0.0	0	0	0	0	Facilities	RBuchanan	01	0089	010089	LAIN
90	Lagerstroemia	indica	Crape myrtle	3.0	8.0	0.0	0	0	0	0	Facilities	RBuchanan	01	0090	010090	LAIN
91	Lagerstroemia	indica	Crape myrtle	3.0	9.0	0.0	0	0	0	0	Facilities	RBuchanan	01	0091	010091	LAIN
92	Lagerstroemia	indica	Crape myrtle	3.0	9.0	0.0	0	0	0	0	Facilities	RBuchanan	01	0092	010092	LAIN
93	Lagerstroemia	indica	Crape myrtle	3.0	8.0	0.0	0	0	0	0	Facilities	RBuchanan	01	0093	010093	LAIN
94	Lagerstroemia	indica	Crape myrtle	4.0	10.0	0.0	0	0	0	0	Facilities	RBuchanan	01	0094	010094	LAIN
95	Lagerstroemia	indica	Crape myrtle	2.0	11.0	0.0	0	0	0	0	Facilities	RBuchanan	01	0095	010095	LAIN
96	Prunus	pensylvanica	Pin Cherry	7.0	20.0	0.0	0	0	0	0	Facilities	RBuchanan	01	0096	010096	PRPE
97	Prunus	pensylvanica	Pin Cherry	7.0	20.0	0.0	0	0	0	0	Facilities	RBuchanan	01	0097	010097	PRPE
98	Prunus	pensylvanica	Pin Cherry	5.0	18.0	0.0	0	0	0	0	Facilities	RBuchanan	01	0098	010098	PRPE
99	Prunus	pensylvanica	Pin Cherry	4.0	15.0	0.0	0	0	0	0	Facilities	RBuchanan	01	0099	010099	PRPE
100	Prunus	pensylvanica	Pin Cherry	6.0	11.0	0.0	0	0	0	0	Facilities	RBuchanan	01	0100	010100	PRPE
101	Prunus	pensylvanica	Pin Cherry	3.0	16.0	0.0	0	0	0	0	Facilities	RBuchanan	01	0101	010101	PRPE

Figure 9 Screen capture of tree inventory attribute table in ArcGIS after field data was collected and keyed as values into the table

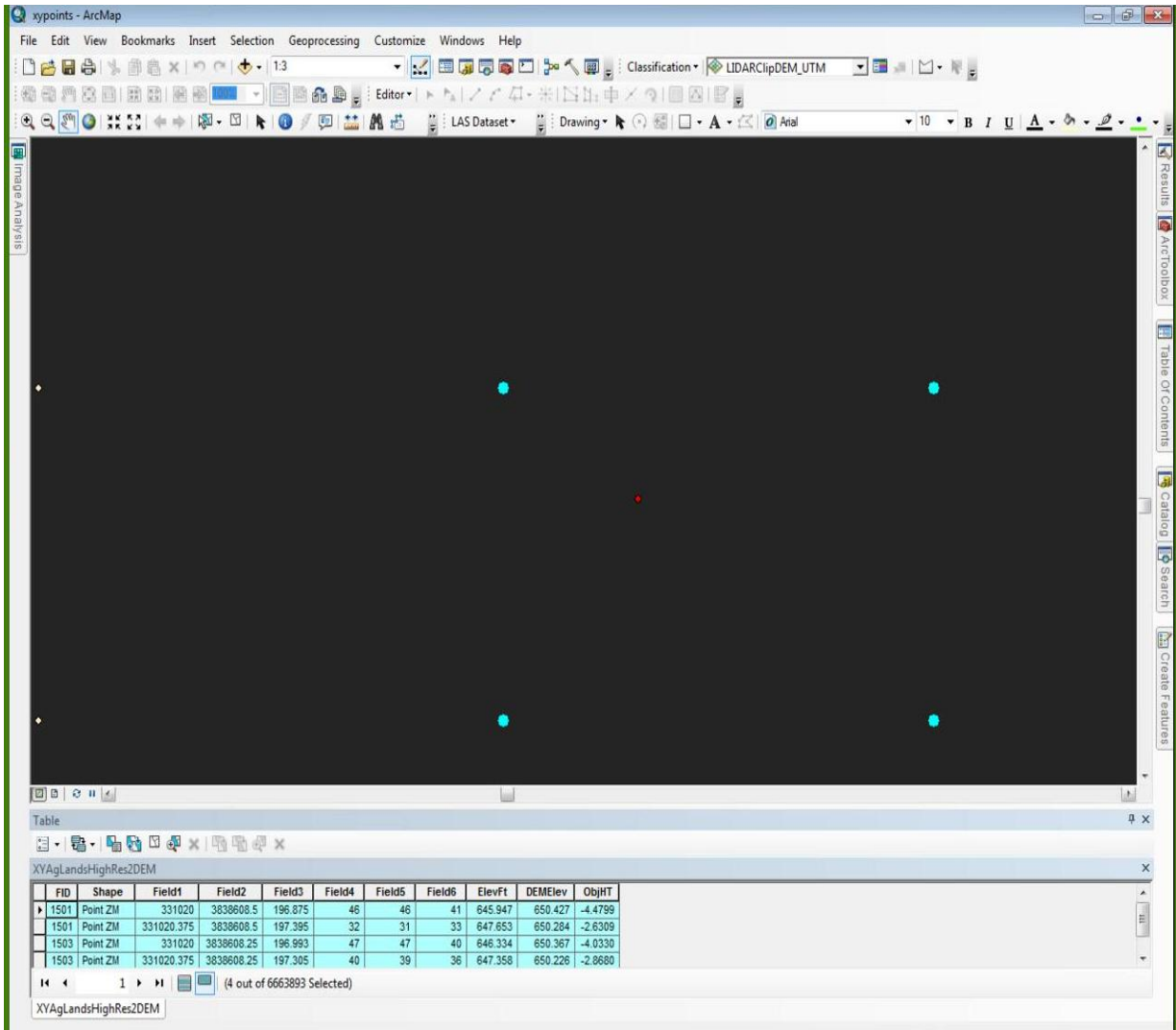


Figure 10 Spatial comparison of Dronemapper point cloud (blue) with tree inventory (red)

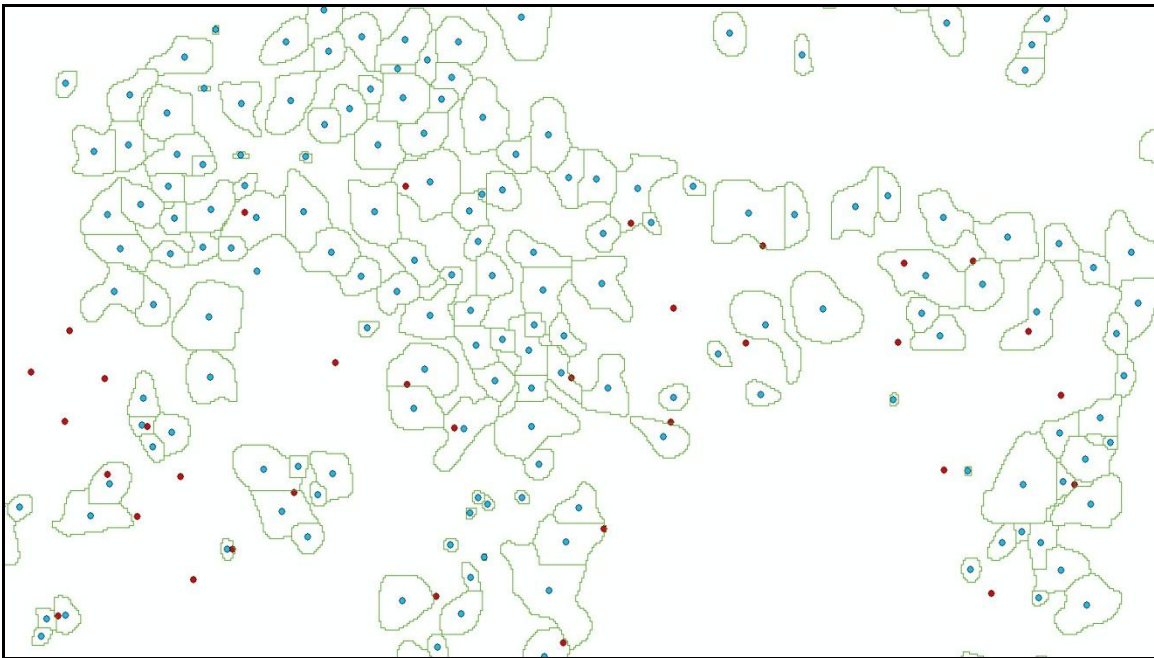


Figure 11 TiFFS output using LiDAR point cloud showing trees (blue) and canopy (green) Trees (red) identified during UAV inventory process are shown for spatial comparison

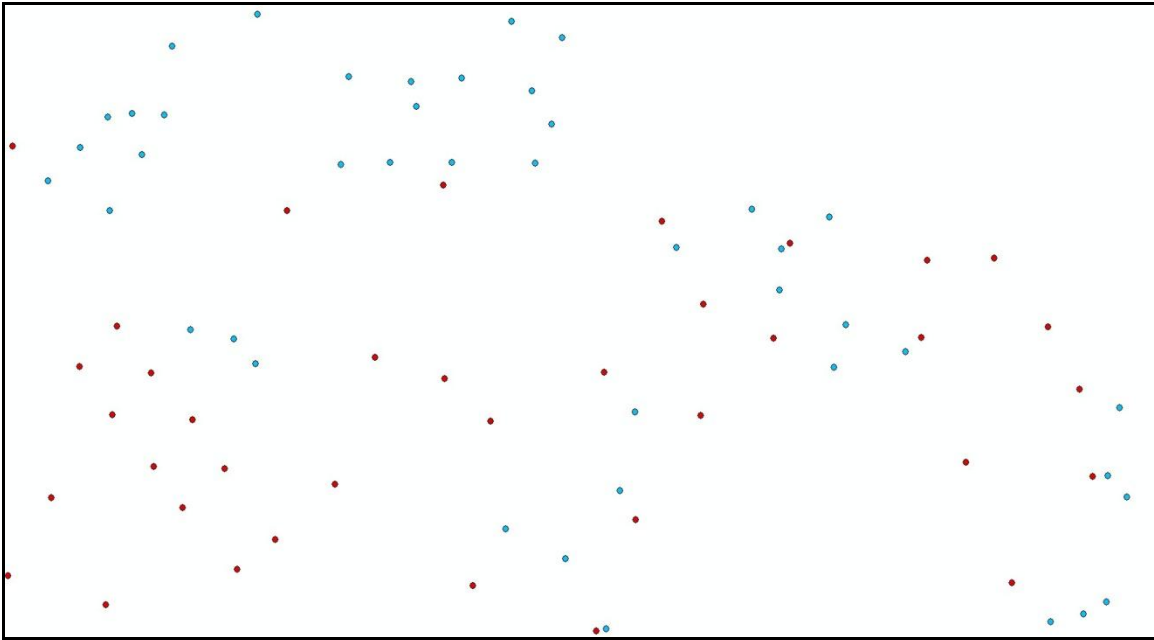


Figure 12 UAV point cloud (DroneMapper) results (blue) using TiFFS showing spatial inaccuracies when compared to tree inventory (red) results

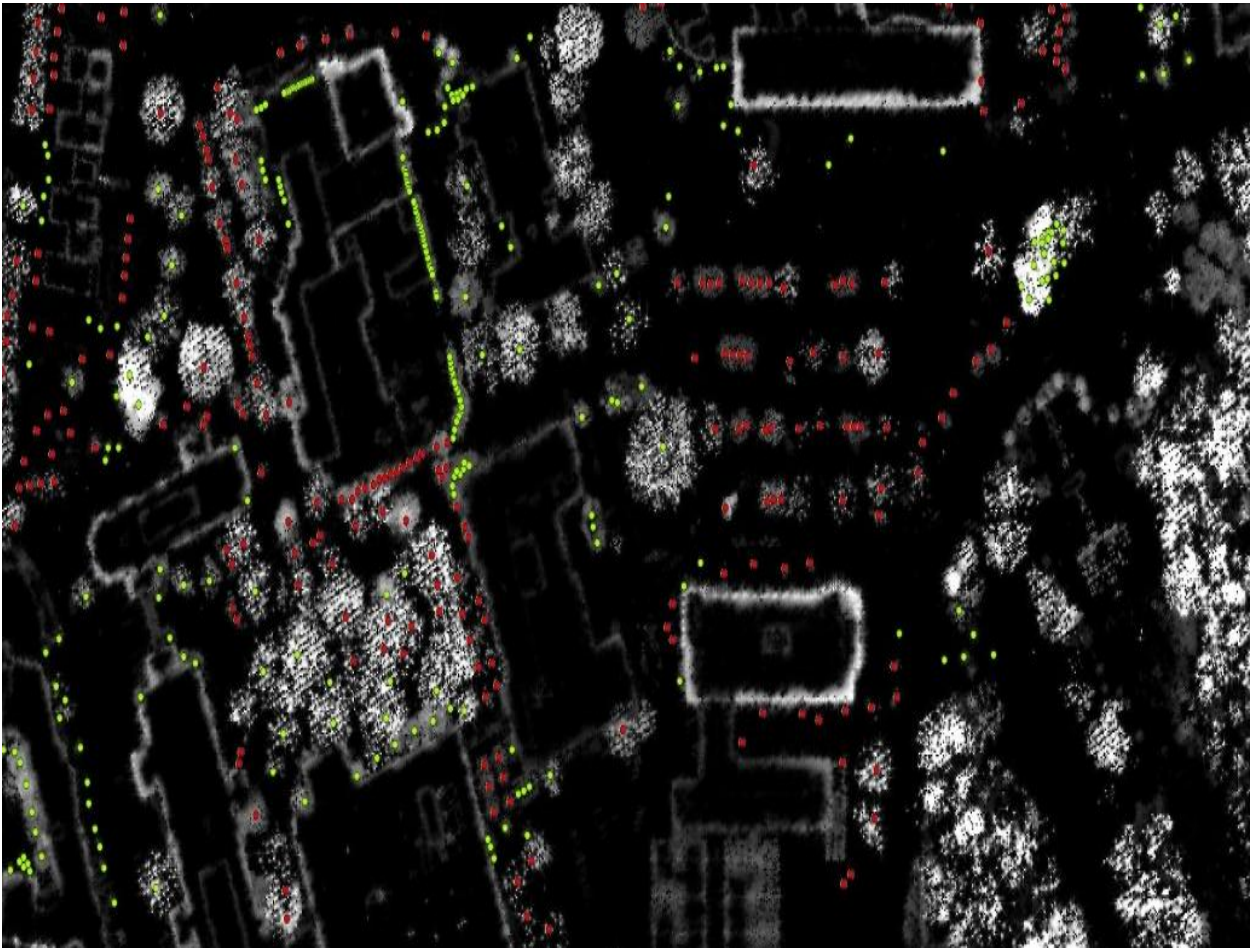


Figure 13 Fusion canopy height model (CHM) results with UAV tree inventory (measured trees -red, unmeasured trees-green) used for spatial comparison

Table 1 Unmanned aerial vehicle (UAV) products related to Urban Forestry uses

UAV products	Urban forestry uses
Color aerial photography	<ul style="list-style-type: none"> - Land cover/use mapping - Tree inventory - Historical documentation - Vegetation analysis (crown density) - Temporal comparison - Planning - Maintenance - Planting - Wildlife corridors - Landscape fragmentation
Near Infrared (NIR) photography	<ul style="list-style-type: none"> - Vegetation analysis - Tree monitoring - Vegetation health monitoring (e.g. insect/disease detection)
LiDAR	<ul style="list-style-type: none"> - Tree heights - Topographic analysis - Watershed analysis - Infrastructure analysis - Soil moisture, - Forest structure - Riparian analysis
DEM	<ul style="list-style-type: none"> - 3D modeling - Contours - Road/trail design - Slope/aspect - Elevation
Thermal imaging	<ul style="list-style-type: none"> - Vegetative analysis, - Insect/disease monitoring - Drought sensitivity

Note: Digital elevation model (DEM) is a product of color images and is used to support other analysis. Technology for LiDAR sensors are creating smaller packages which in time can be incorporated into a UAV platform.

Table 2 Benefits for having a tree inventory (adapted from NCFS, 2014)

Benefits	Examples
Liability Mitigation	Maintenance
	Complaints
	Site visits
	Tree inspection
Budget Considerations	Economic value
	Value-engineered budget allocations
	Budget awareness for maintenance and planting
Planning	Estimated potential
	Future strategies
	Diversity allocation

Table 3 American Society of Photogrammetry and Remote Sensing (ASPRS) Standard
LiDAR Point Classes (ESRI, 2014)

Classification Code	Classification type
0	Never classified
1	Unassigned
2	Ground
3	Low Vegetation
4	Medium Vegetation
5	High Vegetation
6	Building
7	Noise
8	Model Key
9	Water
10	Reserved for ASPRS Definition
11	Reserved for ASPRS Definition
12	Overlap
13–31	Reserved for ASPRS Definition

Table 4 Aerial coverage by UAV flights in summer of 2013

Flight	Number of photos	Date
F01	401	7/17/2013
F02	337	7/17/2013
F03	110	7/17/2013
F001	153	7/17/2013
F002	73	7/17/2013
F01	204	7/19/2013
F02	161	7/19/2013
F01	240	10/1/2013
F02	95	10/1/2013
F01	59	10/2/2013
F02	189	10/2/2013
F01	245	10/3/2013
F02	256	10/3/2013
F01	208	10/4/2013
F02	259	10/4/2013
F01	100	10/18/2013
F02	82	10/18/2013
F01	107	10/29/2013
F02	167	10/29/2013
Total	3446	-----

Table 5 Comparative analyses between UAV and field tree inventory techniques for summer 2013 flight mission

Parameter	UAV image	Field identification
Total trees identified: 6700	5360	1340
Identification time per tree	22.8 sec/tree	2.1 min/tree
Total tree time cost	5.3 days	29.3 days

Table 6 Flow design of processing UAV point cloud using LASTools to classify points into ground and high vegetation to produce DTM and DEM models

Step	Input File	Tool	Output File
1	pointcloud.txt	TXT2LAS	pointcloud.las
2	pointcloud.las	LAS2LAS	pointcloud_prj.las
3	pointcloud_prj.las	LASTILE	Multiple _temp.las files
4	Multiple las Files	LASGROUNDPRO	Multiple _tile_g.las files
5	Multiple _tile_g.las files	LASHEIGHTPRO	Multiple _temp_g_h.las Files
6	Multiple _temp_g_h.las Files	LASCLASSIFYPRO	Multiple _temp_g_h_c.las Files
7	Multiple _temp_g_h_c.las Files	LAS2DEMPRO	Multiple _temp_DEM Files
8	Multiple _temp_g_h_c.las Files	LAS2DEMPRO	Multiple _temp_DTM Files
9	Multiple _temp_DEM Files	Mosaic	pointcloud_DEM
10	Multiple _temp_DTM Files	Mosaic	pointcloud_DTM
11	pointcloud_DEM treeinventory feature class	Extract Values to Points	TreePoints_DEM
12	pointcloud_DTM TreePoints_DEM	Extract Values to Points	TreePoints_DEM_DTM

Table 7 Statistical results of LiDAR comparing measured and estimated tree heights based on tree inventory location to closest LiDAR point. LiDAR data comparison was calculated using all (Composite) and tiled points

Heights (m)	Mean	Std Dev	n	p
Measured	10.005464	6.416815	1831	-----
Composite				
LIDAR < 3.05	12.814899	9.705101	12286	<0.0001
LIDAR < 1.52	8.249866	6.618261	818	<0.0001
LIDAR < 2.44	8.702054	7.465525	1843	<0.0001
Tiled				
4043-02 LIDAR < 2.44	9.435164	8.139745	957	0.0428
4043-01 LIDAR < 2.44	10.867264	1.697426	16	0.5875
4044-04 LIDAR < 2.44	8.734319	7.353198	419	0.0004
4054-03 LIDAR < 2.44	8.421214	7.447031	163	0.0029
4053-01 LIDAR < 2.44	6.508336	4.257981	299	0.0001

Table 8 Statistical comparison of grass and building values to develop a scale factor for pixel conversion to actual elevation heights

	Mean	Std Dev	n	p
Grass	3.59688	0.733275	407	0.056
Building	3.810796	2.123046	380	-----

Table 9 Statistical results of comparing measured and estimated tree heights using Agisoft/LASTool point cloud analysis interpolated to tree inventory points

Heights(m)	Mean	StdDev	n	p
Measured	9.997911	6.395687	1814	-----
Estimated	10.066329	7.303170	1814	0.7641

Table 10 Comparison of means for individual tree species that have measured and estimated heights

Species	% of Total	Measured Heights (m)			Estimated Heights (m)			
		Mean	StdDev	n	Mean	StdDev	n	p
<i>Acer ginnala</i>	1.28	4.37605719	0.75198153	14	4.3899488	1.22707024	14	0.972
<i>Acer nigrum</i>	6.59	13.8091335	4.15245774	72	12.863055	4.60020711	72	0.197
<i>Acer palmatum</i>	0.73	3.8862	1.04201946	8	6.4467705	2.93613941	8	0.036
<i>Acer rubrum</i>	9.33	8.91390587	4.32538053	102	7.7796987	4.52671678	102	0.069
<i>Acer saccharinum</i>	0.18	11.8872	1.8288	2	16.115983	4.98739333	2	0.378
<i>Aquifolaceae</i>								
<i>illex</i>	12.35	6.95621327	2.62169118	135	7.9871215	3.85926726	135	0.011
<i>Betula nigra</i>	1.10	11.7094001	3.90425361	12	13.637374	3.56710823	12	0.22
<i>Carya illinoensis</i>	1.37	18.57248	8.54996461	15	16.562615	8.05530561	15	0.513
<i>Cedrus deodara</i>	1.65	13.5974666	7.54727228	18	12.119252	7.07711158	18	0.573
<i>Cercis canadensis</i>	0.37	8.4582	1.72925323	4	5.4733908	1.75409657	4	0.052
<i>Cornus florida</i>	4.30	7.24386674	2.58647641	47	12.69317	6.6115884	47	0.0001
<i>Cupressus x leylandii</i>	1.92	9.28914271	3.01534068	21	10.650126	3.00641278	21	0.151
<i>Fagus grandifolia</i>	0.64	5.74765719	4.21219488	7	7.1562748	4.22674969	7	0.544
<i>Ginkgo biloba</i>	1.28	9.2964	4.15332428	14	8.7577672	4.15367998	14	0.734
<i>Juniperus virginiana</i>	0.27	16.1544	4.66254358	3	14.178036	4.07077716	3	0.61
<i>Ilex opaca</i>	10.43	7.01842112	2.01473227	114	10.293291	5.46253477	114	0.0001
<i>Lagerstroemia indica</i>	31.11	5.70872478	1.72064812	340	7.3093856	4.40564077	340	0.0001
<i>Liquidambar styraciflua</i>	0.18	21.336	2.7432	2	15.552559	3.36119236	2	0.2
<i>Magnolia grandiflora</i>	4.12	10.24128	4.03872466	45	13.169164	9.51982358	45	0.061
<i>Magnolia x soulangeana</i>	0.46	7.0104	1.27870763	5	5.841955	1.09522382	5	0.159
<i>Magnolia virginiana</i>	2.29	3.47472	0.58775041	25	7.6909931	4.6599284	25	0.0001
<i>Quercus alba</i>	12.90	18.6187403	8.62923736	141	14.882221	10.463966	141	0.001
<i>Quercus coccinea</i>	1.83	12.55776	3.45191883	20	13.020363	5.22263827	20	0.743
<i>Quercus falcata</i>	0.27	15.4432001	4.23319773	3	14.944955	2.61896261	3	0.871
<i>Quercus glauca</i>	0.27	6.4008	1.08479112	3	8.4583036	2.62126119	3	0.277
<i>Quercus macrocarpa</i>	0.82	10.0584	3.01394317	9	10.048625	3.80715012	9	0.995
<i>Quercus</i>	0.82	13.3434667	1.01373981	9	13.370267	2.23069831	9	0.974

palustris

<i>Quercus nigra</i>	1.10	17.653001	3.3399792	12	14.687491	6.12000513	12	0.1548
<i>Quercus virginiana</i>	0.73	13.4112	2.23981335	8	14.455445	3.80807519	8	0.5147
<i>Parrotia persica</i>	0.55	4.0132001	1.22448036	6	4.7621269	1.87422465	6	0.432
<i>Pinus taeda</i>	11.71	5.5387875	1.34494036	128	4.2771447	1.60987801	128	0.0001
<i>Pinus virginiana</i>	0.27	14.2240001	0.57473637	3	15.729783	0.83668149	3	0.062
<i>Prunus pensylvanica</i>	3.02	6.14218177	2.39544332	33	14.243165	21.635794	33	0.036
<i>Prunus x yedoensis</i>	2.20	5.6134001	1.34572065	24	7.0661031	3.83576231	24	0.087
<i>Pyrus calleryana</i>	0.37	12.192	1.27506984	4	17.183432	6.05538967	4	0.158
<i>Taxodium distichum</i>	4.12	8.2499201	4.04587466	45	8.4800145	5.11828237	45	0.814
<i>Thuja occidentalis</i>	1.19	5.55673839	0.2714241	13	3.2774434	0.87714734	13	0.0001
<i>Thuja spp.</i>	0.18	5.4864	0.6096	2	3.0650798	0.56440791	2	0.054
<i>Tilia heterophylla</i>	0.27	13.8175999	2.72999789	3	12.536152	4.51010945	3	0.695
<i>Ulmus parvifolia</i>	5.03	8.23514187	1.3809473	55	7.2475688	1.50065567	55	0.0005
Unknown	1.56	8.44475283	3.28073949	17	6.9956836	3.35958546	17	0.212
Total	100.00			1093				

Note: Species with p shown in red have measured heights \neq estimated heights.

APPENDIX

Glossary

American Standard Code (ASCII):

code that is used for information exchange and is based on the English alphabet using 128 specified characters, 0-9 numbers, letters a-z, and letters A-Z

Agisoft:

a commercial based 3D reconstruction software that uses digital photos. The professional edition allows authoring of geographic information system (GIS) data to produce seamless imagery and 3D point clouds

ArcGIS:

a commercial based geographic information system (GIS) developed by Environmental Systems Research Institute

Autonomous:

operation of a UAV by onboard computer or ground based pilot by remote control

Canopy:

uppermost layer of the forest formed by tree crowns

Canopy Height Model (CHM):

raster based model representing the canopy elevation of the forest and or trees

Diameter at Breast Height (DBH):

measurement location to obtain tree diameter usually at 4.5' off the ground

Digital Elevation Model (DEM):

raster based model representing ground or surface elevations

Digital Terrain Model (DTM):

raster based model representing vegetation height elevations

DroneMapper:

commercial based software for geo-spatial mapping of aerial imagery to produce orthomosaic, digital elevation and digital surface models

Federal Aviation Administration (FAA):

government agency charged with the primary responsibility for safety, advancement and regulation related to civil aviation

Fusion:

free software developed by the United States Forest Service to view and analyze LiDAR data

Geodetic Control Point (GCP):

global positioning system (GPS) derived point that can be used to accurately position non-spatially referenced geographic data by serving as reference object that can be tied to its complimentary location in geographic data

Geographic Information System (GIS):

a computer based software that captures, manages, analyzes, edits and displays geographic data

Geotagging:

process of adding geographic metadata to photographs or imagery

Global Positioning System (GPS):

satellite based navigation system that provides locational information

Ground Control Station:

facilities and computer hardware that maintains human control over unmanned aerial vehicles during flight

Heads-Up-Digitizing:

GIS process for creating feature objects from data (i.e. imagery) displayed on a computer screen

Hyperspectral:

imaging technique that collects data by scanning objects across the electromagnetic spectrum using three techniques: scanning spatial images, sequential capture of full spectral data, or capture spatial and spectral data at the same time

Imagery:

images representing spatial objects on the earth's surface

LASTools:

toolset developed by Martin Isenburg for LiDAR las formatted data. Can be used through DOS command window and as a toolkit or pipeline in ArcGIS

Light Detection and Ranging (LiDAR):

remote sensing technique that uses a laser to measure distance by analyzing reflected light of a laser illuminated object on the earth

Log ASCII Standard (LAS):

standard file format for exchanging LiDAR data

Mosaic:

process of creating a single image from a collection of images

Multi-Spectral:

process of capturing image data at specific frequencies of the electromagnetic spectrum

Multi-Temporal:

data that contains information which spans across different time ranges i.e. multiply years

National Airspace System (NAS):

constitutes the facilities, systems, equipment, procedures, and airports for a flying environment that is safe and efficient

Near Infrared (NIR):

image data collected in the near infrared region of the electromagnetic spectrum this is closest to the radiation detected by the human eye

Orthomosaic:

combination of orthorectification and mosaicing to create a rectified image with limited distortion to form a single image from a collection of images

Orthorectification :

process of correcting imagery distortion by using based data such as elevation along with camera metadata to match map projection

Photogrammetry:

the scientific process(s) of developing measurements from photographs

Point Cloud:

consists of data points referenced to a coordinate system so that each point contains a value for the x, y, and z

Random Access Memory (RAM):

a type of computer data storage for accessing and writing data at the same speed regardless of the order it is accessed

Spatialtemporal:

term used to describe spatial data over a period of time

Soil Type:

defines a soil based upon the soil texture or the size of minerals contained within a soil sample

Soil Volume:

the amount of soil available for a plant to grow into

Structured Query Language (SQL):

programming language used to managing data within a relational database

Toolbox for LiDAR Data Filtering and Forest Studies (TiFFS):

commercial based computer software for automatic viewing and analysis of LiDAR point clouds

Urban Forest:

a collection of trees or forest stands within a city, town or suburb

Unmanned Aerial Vehicle (UAV):

term used to describe a remotely operated airborne vehicle that is flown in absence of a human pilot

Unmanned Aerial System (UAS):

ground control equipment, communication system and other support equipment including the unmanned aerial vehicle to maintain flight mission objectives

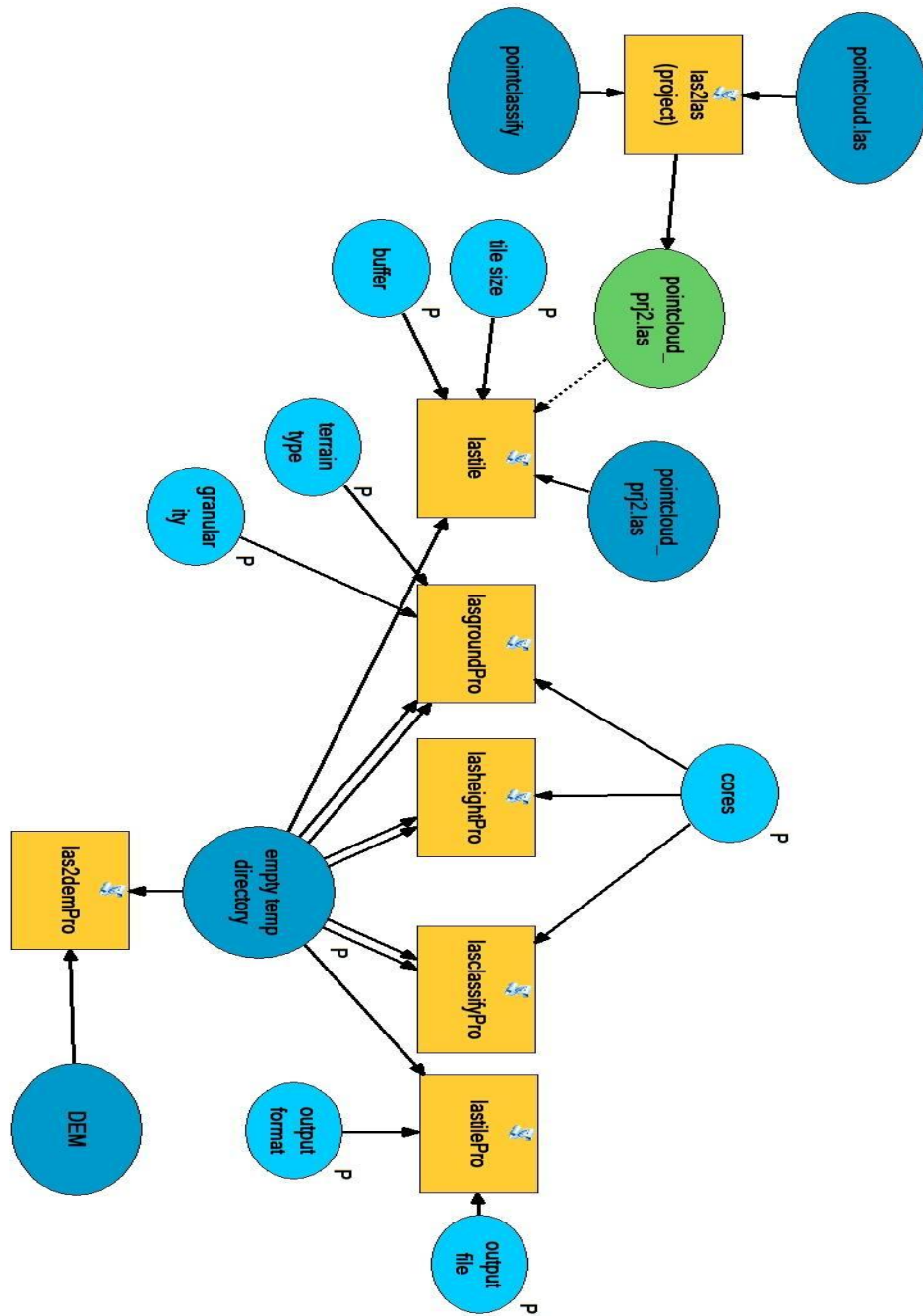
X,Y:

coordinate pair point representing values of a map projection that spatially locates an object on the earth's surface

Z-Value:

spatial value of a map projection that represents elevation of a located object

Flow Diagram for LASTool Batch Processing



REFERENCES

- American Society for Photogrammetry and Remote Sensing (ASPRS), 2012. LASer (LAS) File Format Exchange Activities. Available online at <http://www.asprs.org/Committee-General/LASer-LAS-File-Format-Exchange-Activities.html>
- Anderson, Karen, Gaston, Kevin, 2013. Lightweight unmanned aerial vehicles will revolutionize spatial ecology. *Front Ecol Environ* 11; 11(3): 138-146, doi: 10.1890/120150, March 18 2013.
- Arjomandi, M. 2007. *Classification of Unmanned Aerial Vehicles*. The University of Adelaide, Australia.
- Black, Justin, 2014. Measuring Tree Volume with a Biltmore Stick. Utah State University. Available online at <http://forestry.usu.edu/htm/rural-forests/forest-management/forest-timber-management/measuring-tree-volume-with-a-biltmore-stick/>
- Blom, John David, 2010. Unmanned Aerial Systems: A Historical Perspective. Occasional Paper 37, Combat Studies Institute Press. US Army Combined Arms Center, Fort Leavenworth Kansas.
- Chen, Qi, 2007. Airborne LiDAR Data Processing and Information Extraction. *Journal of Photogrammetric Engineering and Remote Sensing*, February, 2007.
- Clemson, 2013. Clemson University Website History Page; <http://www.clemson.edu/about/history/> About the Clemson University Land Use Property Page; <http://www.clemson.edu/administration/public-affairs/landuse/about.html> Graduate School Information page; <http://www.grad.clemson.edu/GeneralInformation.php>
- DIY, 2013. DIY Drones website by Chris Anderson. <http://diydrones.com/>
- Elias, B. 2012. *Pilotless Drones: Background and Considerations for Congress Regarding Unmanned Aircraft Operations in the National Airspace System*. CRS Report for Congress, Congressional Research Service 7-5700, September 10, 2012.
- Ellison, M. J. (2005). Quantified tree risk assessment used in the management of amenity trees. *Journal of Arboriculture*, 31(2), 57-654. Available online at <http://www.qtra.co.uk/docs/QTRA.pdf>

- Environmental Systems Resource Institute (ESRI), 2014. Online ArcGIS Resource Center. Help Desk ArcGIS version 10.2. Available online at <http://resources.arcgis.com/en/help/main/10.2/index.html#/00qn0000001p000000>
- Eugster, H., & Nebiker, S. (2008). UAV-Based Augmented Monitoring-Real-Time Georeferencing and Integration of Video Imagery with Virtual Globes. *IAPRSSIS*, 37(B1), 1229-1235.
- Forest Resource Assessment Nepal, 2014. LiDAR Assisted Multisource Programme in TAL. Available online at http://www.franepal.org/?page_id=135
- GAO, 2012. *Measuring Progress and Addressing Potential Privacy Concerns Would Facilitate Integration into the National Airspace System* US Accountability Office report to Congress. [Reissued on September 18, 2012] GAO-12-981, Sep 14, 2012 Available online at <http://www.gao.gov/assets/650/648348.pdf>
- Globalidar, 2014. TIFFS, The Lidar Information Engine. Available online at <http://www.globalidar.com/Pages/default.aspx>
- Harwin, S., Lucieer, A. 2012. Assessing the accuracy of georeferenced point clouds produced via multi-view stereopsis from unmanned aerial vehicle (UAV) imagery. *Remote Sensing*, 4(6), 1573-1599.
- Hunt, E. R., Hively, W. D., Fujikawa, S. J., Linden, D. S., Daughtry, C. S., & McCarty, G. W. (2010). Acquisition of NIR-green-blue digital photographs from unmanned aircraft for crop monitoring. *Remote Sensing*, 2(1), 290-305.
- International Society of Arboriculture 2013. Using the ISA Basic Tree Risk Assessment Form. Available online at http://www.isa-arbor.com/education/resources/isabasictreeriskassessmentform_instructions.pdf
- Jomaa Ihab, Auda Yves, Saleh Bernadette Abi, Hamze, & Safi, Samir, 2008. Landscape spatial dynamics over 38 years under natural and anthropogenic pressures in Mount Lebanon. *Landscape and Urban Planning*, 87: 67-75.
- Johnston, L. F., Herwitz, S., Dunagan, S., Lobitz, B., Sullivan, D., Slye, R., 2003. Collection of Ultra High Spatial and Spectral Resolution Image Data over California Vineyards with a Small UAV. Proceedings, International Symposium on Remote Sensing of Environment, 2003. Available online at <http://www.uav-applications.org/gallery/img/5.pdf>

- Laliberte, A. S., Winters, C., & Rango, A. 2008. *A procedure for orthorectification of sub-decimeter resolution imagery obtained with an unmanned aerial vehicle (UAV)*. In Proceedings of ASPRS Annual Conference (p. 9) April 2008.
- Merino, L., Caballero, F., Martinez-de Dios, J. R., Ferruz, J., Ollero, A. 2006. *A cooperative perception system for multiple UAVs: Application to automatic detection of forest fires*. *Journal of Field Robotics*, Vol. 23, Iss. 3-4, March-April 2006 pp. 165-184, Available online at <http://www3.interscience.wiley.com/cgi-bin/jhome/111090262> Wiley Periodicals Inc.
- Mitchell, M. 2012. *President Obama Signs The FAA Modernization And Reform Act Of 2012 (H.R. 658)*. Aviation Online Magazine, February 15, 2012. Available online at http://avstop.com/news_february_2012/president_obama_signs_the_faa_modernization_and_reform_act_of_2012_hr_658.htm
- National Oceanic and Atmospheric Administration (NOAA), 2013. LIDAR—Light Detection and Ranging—is a remote sensing method used to examine the surface of the Earth. Available online at <http://oceanservice.noaa.gov/facts/lidar.html>
- North Carolina Forest Service (NCFS) 2014. Urban and Community Tree Inventories. Available online at http://www.ncforestsERVICE.gov/Urban/urban_tree_inventories.htm
- Pokorny, Jill; O'Brien, Joseph; Hauer, Richard; Johnson, Gary; Albers, Jana; Bedker, Peter; Mielke, Manfred 2003. *Urban Tree Risk Management: A Community Guide to Program Design and Implementation*. USDA Forest Service Northeastern Area State and Private Forestry 1992 Folwell Ave. St. Paul, MN 55108
- Pudelko, Rafal, Stuczynski, Tomasz, Borzecka-Walker, Magdalena, 2012, The suitability of an unmanned aerial vehicle (UAV) for the evaluation of experimental fields and crops. *Zemdirbyste=Agriculture*, vol. 99, No. 4, 2012, p. 431-436.
- Rango, A., and Laliberte, A. S. 2010. Impact of flight regulations on effective use of unmanned aircraft systems for natural resources applications. *Journal of Applied Remote Sensing*, 4(1), 043539-043539.
- Rapidlasso, 2014. Creator of LASTools for LiDAR. <http://rapidlasso.com/>
- Remondino, F., Barazzetti, L., Nex, F., Scaioni, M., & Sarazzi, D. 2011. *UAV photogrammetry for mapping and 3D modeling—current status and future perspectives—*. Proceedings of the International Archives of the Photogrammetry, Remote Sensing and Spatial Information Sciences, 38, 1.

- Rowntree, R. A. 1988. Ecology of the Urban Forest: Introduction to Part III. *Landscape Urban Plann.*, 15:1-10.
- Rudol, P., & Doherty, P., 2008. Human body detection and geolocalization for UAV search and rescue missions using color and thermal imagery. In *Aerospace Conference, 2008 IEEE* (pp. 1-8). IEEE.
- United States Forest Service (USFS), 2014. LIDAR & IFSAR Tools.. U.S. Department of Agriculture, Pacific Northwest Research Station. Available online at http://forsys.cfr.washington.edu/JFSP06/lidar_&_ifsar_tools.htm
- Wallace, L., Lucieer, A., Watson, C., & Turner, D., 2012. Development of a UAV-LiDAR system with application to forest inventory. *Remote Sens*, 4(6), 1519-1543.
- Wang, Yunsheng; Weinacker, Holger; Koch, Barbara. 2008. "A Lidar Point Cloud Based Procedure for Vertical Canopy Structure Analysis And 3D Single Tree Modeling in Forest." *Sensors* 8, no. 6: 3938-3951.
- Yunfei, B., Guoping, L., Chunxiang, C., Xiaowen, L., Hao, Z., Qisheng, H., ... & Chaoyi, C., 2008. Classification of LIDAR point cloud and generation of DTM from LIDAR height and intensity data in forested area. In *ISPRS Congress*
- Zhou, Xiaolu, Wang, Yi-Chen, 2011. Spatial-temporal dynamics of urban green space in response to rapid urbanization and greening policies. *Landscape and Urban Planning*, 100 (2011); 268-277.